JOURNAL OF GEOPHYSICAL RESEARCH, VOL. 96, NO. A4, PAGES 5825–5836, APRIL 1, 1991

Electrostatic Noise in Non-Maxwellian Plasmas: Generic Properties and "Kappa" Distributions

YVES F. CHATEAU[1] AND NICOLE MEYER-VERNET

Recherche Spatiale, Observatoire de Paris, Meudon, France

We study the generic properties of the electrostatic noise spectrum measured by an antenna immersed in a plasma with an isotropic electron velocity distribution function, at frequencies of the order of magnitude of the plasma frequency. We find that at high frequencies the noise level is proportional to the electron pressure for long wire antennae and to the electron flux for long double-sphere antennae. At low frequencies it depends mostly on the low-energy electrons. We also study the shape of the peak near the plasma frequency, for distribution functions with Maxwellian or power law high-energy tails. We calculate the noise produced with a generalized Lorenzian ("kappa") distribution function and compare the results with those obtained with different distributions having the same density and equivalent temperature. We deduce some practical consequences for plasma wave measurements in space.

1. INTRODUCTION

Although the conventional use of electric antennae is for remote sensing by detection of electromagnetic waves, they can also be used for in situ measurements, by detecting electrostatic waves produced by the random motion of the ambient plasma particles. The spectroscopy of this quasi-thermal noise near the plasma frequency is currently used for measuring electron parameters in space plasmas [see *Meyer-Vernet and Perche*, 1989 and references therein]. It is also planned to be used on future missions such as Ulysses and Wind in the solar wind, and CRAF and Cassini in a cometary and the Saturnian environment, respectively.

This method is complementary to conventional electron analyzers; in effect, since it "sees" a much larger plasma volume, it is less sensitive to spacecraft and secondary particle perturbations, so that it works better than conventional analyzers at low temperatures; in any case, it becomes less efficient when the temperature is so high that the Debye length becomes larger than the antenna length.

This method has been studied for realistic antenna geometries by using a simple model of velocity distribution, made of two Maxwellians [see *Meyer-Vernet and Perche*, 1989 and references therein]. More recently, it has been extended to flat-top distributions [*Chateau and Meyer-Vernet*, 1989]. The aim of this paper is to study more general distribution functions, and to derive some generic properties of the quasi-thermal noise as a function of the electron velocity distribution.

More precisely, we will try to answer the following questions: What are the model independent properties of this noise, if they exist at all? Can one deduce global plasma properties from the noise spectrum detected by a given antenna, without taking a particular model for the distribution function?

As an illustration, we will calculate the noise produced with generalized Lorenzian ("kappa") distributions [*Vasyliunas*, 1968; *Olbert*, 1968]. This form has the advantage of being analytically tractable, while representing rather well the electron distribution in different media such as the solar wind or planetary magnetospheres; indeed, it is not very different from a Maxwellian at low energies but has a high-energy tail with a power law form. Therefore these calculations can be easily used to generalize the theory and its applications to distribution functions having a power law tail.

We will compare the results obtained with different distribution functions, in order to illustrate the generic properties of the noise, and finally deduce some practical consequences for plasma measurements in space.

Unless otherwise stated, we shall use SI units.

2. BASICS

We study the following problem. An electric dipole antenna is at rest in a homogeneous infinite plasma. The antenna is assumed to be gridlike and at zero dc potential and is defined by its current distribution $\mathbf{J}(\mathbf{r})$. We will consider either thin cylindrical wire dipoles of tip-to-tip length $2L$ or dipoles made of two small spheres separated by L, of radius a much smaller than the Debye length; we assume $\omega L/c \ll 1$. The plasma is defined by the electron velocity distribution $f(v)$, assumed isotropic, and by the (angular) plasma frequency $\omega_p = (ne^2/\varepsilon_0 m)^{1/2}$, n being the electron density. The ions are assumed to be stationary, since we restrict our analysis to frequencies of the order of magnitude of ω_p.

We then calculate the power spectrum V^2 of the voltage at the antenna terminals. From Nyquist's theorem this quantity would be $4k_BTR$ in the special case of thermal equilibrium, R being the antenna resistance; note that in practice, R only involves the electrostatic part of the field, since this contribution is generally much larger than the electromagnetic part [see *Couturier et al.*, 1981] (and the space plasma involved is generally optically thin for electromagnetic waves). For nonequilibrium but stable distribution functions, V^2 is calculated by using the correlation tensor of the electric field fluctuations in the plasma, $E_{ij}(\mathbf{k}, \omega)$ in Fourier space, which is a known function of $f(v)$ [e.g., *Sitenko*, 1967].

As is well known, this noise can be viewed and calculated

[1]Also at Université Paris 6.

Paper number 90JA02565.
0148-0227/91/90JA-02565$05.00

as the fluctuating electrostatic field due to the motion of passing plasma particles, "dressed" by the dielectric function $\varepsilon_L(\mathbf{k}, \omega)$. Broadly speaking, this means that for $\omega < \omega_p$ the antenna mostly sees the shot noise of electrons passing at distances smaller than the Debye length (see equation (9)), while for $\omega > \omega_p$ the plasma temporal dispersion (i.e., the variation of ε_L with ω) also becomes important and the electron motion induces damped longitudinal plasma waves.

We start from the expression of V^2 deduced [*Chateau and Meyer-Vernet*, 1989] from the correlation tensor $E_{ij}(\mathbf{k}, \omega)$ and the antenna geometry:

$$V^2 = \frac{16m\omega_p^2}{\pi\varepsilon_0}\int_0^\infty dk\,\frac{F(kL)B(k)}{k^2|\varepsilon_L|^2} \tag{1}$$

$$B(k) = \frac{2\pi}{k}\int_{\omega/k}^\infty dv\, vf(v) \tag{2}$$

$$\varepsilon_L = 1 + \frac{2\pi\omega_p^2}{k}\int_{-\infty}^{+\infty} dv_\parallel\,\frac{v_\parallel f(v_\parallel)}{kv_\parallel - \omega - io} \tag{3}$$

where $v_\parallel$ is the component of $\mathbf{v}$ parallel to $\mathbf{k}$ and the distribution function is normalized as

$$\int d^3v\, f(v) = \int dv\, 4\pi v^2 f(v) = 1$$

The term io denotes an infinitesimal positive imaginary part, and the function F specifies the antenna geometry as

$$F(x) = \frac{1}{x}\left[\mathrm{Si}\,(x) - \tfrac{1}{2}\,\mathrm{Si}\,(2x) - \frac{2}{x}\sin^4\left(\frac{x}{2}\right)\right] \quad \text{(wires)} \tag{4}$$

$$F(x) = \frac{1}{4}\left(1 - \frac{\sin x}{x}\right) \quad \text{(spheres)} \tag{5}$$

where Si is the sine integral function; for the wire antenna we have assumed that the current varies linearly with the distance to the antenna feed point [see *Couturier et al.*, 1981].

Note that from (3) the imaginary part of ε_L is

$$\mathrm{Im}\ \varepsilon_L = \frac{2\pi^2\omega\omega_p^2}{k^3} f\left(\frac{\omega}{k}\right) \tag{6}$$

3. Generic Properties of the Electrostatic Noise

We will characterize the noise V^2 in the most general way, i.e., as a function of the (angular) plasma frequency ω_p and of the other moments of the distribution function $f(v)$ defined as

$$\langle v^n\rangle = \int d^3v\, v^n f(v) = \int dv\, 4\pi v^{n+2} f(v) \tag{7}$$

We define the equivalent temperature as

$$T = \frac{m}{3k_B}\langle v^2\rangle \tag{8}$$

We will study the specific cases $\omega \ll \omega_p$ (but still much larger than the ion plasma frequency), $\omega \gg \omega_p$, and $\omega \approx \omega_p$.

3.1. *Low Frequencies*

Let us consider the limit $\omega/kv \to 0$. The dielectric function (3) becomes

$$\varepsilon_L \approx 1 + \frac{4\pi\omega_p^2}{k^2}\int_0^\infty dv\, f(v)$$

which can be rewritten by analogy with a Maxwellian plasma, in the form

$$\varepsilon_L \approx 1 + \frac{1}{k^2L_D^2} \tag{9}$$

where the Debye length is defined as

$$L_D = \left[4\pi\omega_p^2\int_0^\infty dv f(v)\right]^{-1/2} \tag{10}$$

Note in passing that in the particular case where $f(v)$ is Maxwellian, this definition yields the Debye length as a function of the temperature as

$$L_{D_{\mathrm{maxw}}} = \left(\frac{k_BT}{m\omega_p^2}\right)^{1/2} \tag{11}$$

In general, however, $L_D \neq L_{D_{\mathrm{maxw}}}$, although both quantities are of the same order of magnitude. Hereafter, we shall use $L_{D_{\mathrm{maxw}}}$ when we need an expression depending only on ω_p and the equivalent temperature T (8), but not on the particular shape of the distribution.

Taking the low-frequency limit of (2), we deduce from (1) (making the change of variable $y = kL_D$) the variation of the noise with the distribution function $f(v)$,

$$V^2 = \frac{8m}{\pi\varepsilon_0}\left[\int_0^\infty dvvf(v)\right]\left[\int_0^\infty dvf(v)\right]^{-1}\int_0^\infty dy\,\frac{yF(yL/L_D)}{(1+y^2)^2} \tag{12}$$

First, let us consider long antennae, i.e., $L/L_D \gg 1$. The function F can be approximated for large arguments by

$$F(x) \approx \frac{\pi}{4x} \qquad x \gg 1 \quad \text{(wires)} \tag{13}$$

$$F(x) \approx \tfrac{1}{4} \qquad x \gg 1 \quad \text{(spheres)} \tag{14}$$

We thus obtain from (12)

$$V^2 = \frac{\pi^{1/2}m}{4\varepsilon_0\omega_pL}\left[\int_0^\infty dvvf(v)\right]\left[\int_0^\infty dvf(v)\right]^{-3/2} \tag{15}$$

$$L/L_D \gg 1 \quad \text{(wires)}$$

$$V^2 = \frac{m}{\pi\varepsilon_0}\left[\int_0^\infty dvvf(v)\right]\left[\int_0^\infty dvf(v)\right]^{-1} \tag{16}$$

$$L/L_D \gg 1 \quad \text{(spheres)}$$

Second, consider short antennae, i.e., $L/L_D \ll 1$. The function F can be approximated for small arguments by

$$F(x) \approx x^2/24 \qquad x \ll 1 \quad \text{(wires or spheres)} \tag{17}$$

Inserting (17) into the part of the y integral in (12) where $yL/L_D < 1$, we obtain for both the wire and the sphere dipole antennae

$$V^2 = \frac{4m\omega_p^2 L^2}{3\varepsilon_0}\,[\ln (L_D/L) + O(1)] \int_0^\infty dv v f(v) \qquad (18)$$

$$L/L_D \ll 1$$

Looking at (15), (16), and (18), one sees that whether the antenna is made of wires or spheres, and whether it is large or small, the low-frequency noise level depends on the lower moments of the distribution function $f(v)$, and thus mainly on the lower-velocity electrons. We expect, therefore, that it will be nearly insensitive to any high-energy tail of the velocity distribution.

3.2. *High Frequencies*

Let us now consider high frequencies, i.e., $\omega \gg \omega_p$. In this case we can make the approximation $\varepsilon_L \approx 1$ in (1) and thus obtain

$$V^2 \approx \frac{32m\omega_p^2}{\varepsilon_0} \int_0^\infty dk\, \frac{F(kL)}{k^3} \int_{\omega/k}^\infty dv v f(v) \qquad (19)$$

which can be rewritten

$$V^2 \approx \frac{32m\omega_p^2}{\varepsilon_0} \int_0^\infty dv\, v f(v) \int_{\omega/v}^\infty dk\, \frac{F(kL)}{k^3} \qquad (20)$$

For antennae satisfying $\omega L/\omega_p L_D \gg 1$, we approximate the function F by using (13) or (14) depending on the antenna geometry, and we deduce the noise power spectrum

$$V^2 \approx \frac{2m\omega_p^2}{3\varepsilon_0 L\omega^3} \langle v^2 \rangle \qquad \omega/\omega_p \gg \max\,[1,\, L_D/L] \quad \text{(wires)} \qquad (21)$$

$$V^2 \approx \frac{m\omega_p^2}{\pi\varepsilon_0\omega^2} \langle v \rangle \qquad \omega/\omega_p \gg \max\,[1,\, L_D/L] \quad \text{(spheres)} \qquad (22)$$

where the moments of the distribution function are defined in (7).

We therefore obtain the very interesting result that the high-frequency electrostatic noise is proportional to the total electron pressure P for long wire antennae and proportional to the total electron flux J for long double-sphere antennae:

$$V^2 \approx \frac{2e^2}{\varepsilon_0^2 L m\omega^3} P \qquad \omega/\omega_p \gg \max\,[1,\, L_D/L] \quad \text{(wires)} \qquad (23)$$

$$V^2 \approx \frac{4e^2}{\pi\varepsilon_0^2 m\omega^2} J \qquad \omega/\omega_p \gg \max\,[1,\, L_D/L] \quad \text{(spheres)} \qquad (24)$$

where $P = nm\langle v^2 \rangle/3 = nkT$ and $J = nm\langle v \rangle/4$ and where the equivalent temperature is defined in (8). This generalizes to any stable distribution function, the results previously found [*Meyer-Vernet and Perche*, 1989] for distributions made of a sum of Maxwellians.

3.3. *Frequencies Just Above the Plasma Frequency*

Let us now consider frequencies $\omega \approx \omega_p$.

For short antennae, i.e., $L/L_D \ll 1$, we expect that the noise V^2 will not vary greatly with frequency [*Meyer-Vernet and Perche*, 1989]; indeed, antennae of length L are mostly sensitive to wave numbers $k \geq 1/L$ (see (4) and (5)), i.e., to $k \gg 1/L_D$ for short antennae; this means that the range $\omega/kv \ll 1$ should play the dominant part in the integral (1), so that the results obtained in section 3.1 should hold also for any frequency of the order of magnitude of the plasma frequency.

Let us now consider long antennae, i.e., $L/L_D \gg 1$. We then take the opposite limit $\omega/kv \gg 1$; considering sufficiently well-behaved distribution functions, we use the asymptotic expansion of (3) in powers of kv/ω,

$$\text{Re}\ \varepsilon_L \approx 1 - \frac{\omega_p^2}{\omega^2}\left[1 + \frac{k^2}{\omega^2}\langle v^2 \rangle + \frac{k^4}{\omega^4}\langle v^4 \rangle + \cdots\right] \qquad (25)$$

Hence the nearly real zero of ε_L,

$$k_0 \approx \frac{\omega}{\langle v^2 \rangle^{1/2}} \left(\frac{\omega^2}{\omega_p^2} - 1\right)^{1/2} \qquad (26)$$

which is analogous to the usual Langmuir wave in a thermal plasma.

We now calculate the contribution of this zero to the integral (1) giving the noise. Writing for $k \approx k_0$

$$\text{Re}\ \varepsilon_L \approx (k - k_0)\, \frac{\partial\ \text{Re}\ \varepsilon_L}{\partial k}$$

$$\frac{\partial\ \text{Re}\ \varepsilon_L}{\partial k} \approx -\frac{2\omega_p^2 k_0 \langle v^2 \rangle}{\omega^4}$$

we deduce the contribution to V^2,

$$V_0^2 \approx \frac{16m\omega_p^2}{\varepsilon_0} F(k_0 L) B(k_0) \left(k_0^2 \left| \text{Im}\ \varepsilon_L \frac{\partial\ \text{Re}\ \varepsilon_L}{\partial k} \right|_{k=k_0}\right)^{-1}$$

and hence

$$V_0^2 \approx \frac{4m\omega_p F(k_0 L) B(k_0)}{\pi^2 \varepsilon_0 \langle v^2 \rangle f(\omega/k_0)} \qquad L/L_D \gg 1 \qquad (27)$$

with $B(k)$ given in (2), thus

$$B(k_0) = \frac{2\pi}{k_0} \int_{\omega/k_0}^\infty dv\, v f(v) \qquad (28)$$

Hence when k_0 is given by (26), the noise exhibits a cutoff at $\omega = \omega_p$, with a peak given by V_0^2 just above ω_p. This peak depends, through $B(k_0)/f(\omega/k_0)$, on the distribution function for velocities $v \geq \omega/k_0$. Thus for a given value of ω/ω_p the noise depends on the electrons of velocity

$$v \geq v_\omega = \frac{\omega}{k_0} = \left[\frac{\langle v^2 \rangle}{(\omega^2/\omega_p^2 - 1)}\right]^{1/2} = \left(\frac{3k_B T}{2mX}\right)^{1/2} \qquad (29)$$

where we have put

$$X = \frac{\omega}{\omega_p} - 1 \ll 1$$

so that the high-energy electrons determine the noise near ω_p.

Note that a relativistic treatment would be needed if relativistic electrons contributed much, namely if v_ω were not much smaller than c; this occurs when $X = \omega/\omega_p - 1$ is equal to or smaller than

$$X_m = \frac{\langle v^2 \rangle}{2c^2} \approx 2.5 \times 10^{-10} T(\mathrm{K}) \tag{30}$$

Therefore, in the usual space plasmas this problem occurs only for very small receiver bandwidths; for instance, in the solar wind it only occurs when $\omega/\omega_p - 1$ is smaller than a few times 10^{-4}.

It must also be kept in mind that the approximation (26) of k_0 is not valid for any distribution function; in some cases, the first terms of the asymptotic expansion (25) may not represent a correct estimate (even though a relativistic treatment ensures the convergence of the high-order moments $\langle v^n \rangle$), and other nearly real zeros of ε_L might appear. In practice, however, this problem only occurs in the rare case when the contribution of the very hot electrons to the pressure is dominant.

Now, let us deduce the shape of the peak for different high-energy electron distributions.

First, let us assume that the high-energy tail of $f(v)$ is a Maxwellian whose temperature is $T_H = mv_H^2/2$, such that

$$f(v) \propto \exp(-v^2/v_H^2) \qquad v \geq v_\omega \tag{31}$$

v_ω being defined in (29). In this case, $B(k_0)/f(\omega/k_0) \propto 1/k_0$, and (27) yields

$$V_0^2 \approx \frac{4m\omega_p F(k_0 L) v_H^2}{\pi \varepsilon_0 \langle v^2 \rangle k_0} \qquad L/L_D \gg 1 \tag{32}$$

for frequencies such that (31) holds. Since $F(x) \propto x^2$ for $x \to 0$, one has $V_0^2 \to 0$ when $\omega \to \omega_p$, and the noise has a peak at the value of ω/ω_p corresponding to the value of

$$k_0 L = \left(\frac{2X}{3}\right)^{1/2} \frac{L}{L_{D_{\mathrm{maxw}}}}$$

for which $F(x)/x$ is maximum [*Meyer-Vernet and Perche*, 1989]; the peak occurs at $X = \omega/\omega_p - 1 \approx 8(L_{D_{\mathrm{maxw}}}/L)^2$ for the wire dipole antenna (and a value about 2 times larger for the double-sphere dipole); its width is of the same order of magnitude, defining the "width" as the relative frequency band for which the noise is larger than about $1/e$ its peak value. The amplitude of the peak [*Meyer-Vernet and Perche*, 1989] can be put in the form

$$V_{\max}^2 \approx \frac{0.05(mk_BT)^{1/2}}{\varepsilon_0} \frac{T_H}{T} \frac{L}{L_D}$$

$$\approx 2 \times 10^{-17} (T)^{1/2} \frac{T_H}{T} \frac{L}{L_D} \tag{33}$$

for the wire dipole antenna (and a value about 30% larger for the spheres).

Let us now assume that the high-energy tail of $f(v)$ has a power law shape

$$f(v) \propto v^{-n} \qquad v \geq v_\omega \tag{34}$$

In this case, we expect a more spiky behavior for V_0^2 since $B(k_0)/f(\omega/k_0) \propto 1/k_0^3$, so that (27) yields

$$V_0^2 \approx \frac{8m\omega_p^3 F(k_0 L)}{\pi \varepsilon_0 (n-2) \langle v^2 \rangle k_0^3} \qquad L/L_D \gg 1 \tag{35}$$

for frequencies such that (34) holds.

Equation (35) exhibits an important difference with the Maxwellian case: the function $F(x)/x^3 \to \infty$ when $x \to 0$, without having a maximum at $x \neq 0$. This would yield $V_0^2 \to \infty$ for $\omega \to \omega_p$ if the electron velocities were allowed to become infinite, but as indicated above, equation (35) is not valid too close to ω_p, i.e., for $X \leq X_m$ (X_m being defined in (30)). To obtain the peak behavior, we approximate F by (17) for $k_0 L \ll 1$, and we get

$$V_0^2 \approx \frac{0.04(mk_BT)^{1/2}}{\varepsilon_0 (n-2) X^{1/2}} \left(\frac{L}{L_{D_{\mathrm{maxw}}}}\right)^2 \tag{36}$$

for

$$X_m \ll X = \omega/\omega_p - 1 \ll (L_{D_{\mathrm{maxw}}}/L)^2 \ll 1$$

(and X such that (34) holds, v_ω being given by (29)). Thus the noise has a finite peak at X of the order of X_m and a width (at $1/e$ level) of the same order. In practice, this part will generally be hidden by the finite frequency resolution $\Delta\omega/\omega$ of the receiver, so that the apparent peak amplitude will be of the order of the value given by (36) where X is replaced by $\Delta\omega/\omega$ (assuming the resolution $\Delta\omega/\omega < (L_{D_{\mathrm{maxw}}}/L)^2$ and of the order of the relative bandwidth, so that the noise measured should be of the order of the mean of (36) over the bandwidth $\Delta\omega$). In practice, however, this part of the spectrum might be modified by the antenna impedance as discussed in section 3.4.

In short, for long antennae, while the cutoff of the spectrum occurs at the plasma frequency, the fine structure of the peak just above ω_p depends on the shape of the high-energy tail of the velocity distribution. More precisely, if it is Maxwellian, then the peak occurs above ω_p, and its width is of the order of $8(L_D/L)^2$; on the other hand, for a power law tail the peak is nearly at ω_p and is sharper (and it has also a fine structure of relative width $\langle v^2 \rangle/2c^2$, which is generally hidden by the finite receiver bandwidth).

An important question therefore arises: Consider an experiment having a frequency resolution $\Delta\omega/\omega$ insufficient to resolve the fine structure of the peak. In this case, one cannot deduce the high-energy tail of $f(v)$; more precisely, one cannot deduce $f(v)$ for $v \geq [\langle v^2 \rangle/(2\Delta\omega/\omega)]^{1/2}$, except if these electrons contribute significantly to the pressure or to lower-order moments of $f(v)$. But one can still deduce the plasma frequency and the other low-order moments of $f(v)$, by using the other parts of the spectrum.

3.4. *Antenna Impedance*

The voltage power spectrum calculated above appears at the antenna terminals. In practice, however, the antenna is connected to a receiver with a finite impedance Z_R. It is

possible to build receivers with an input resistance of the order of 10^9 ohms or larger, but one cannot eliminate, in parallel to this resistance, a "base" capacity C_b due to the receiver input capacity and to the antenna erecting mechanism, which is usually of the order of a few tens of picofarads, so that one generally has $Z_R \approx 1/iC_b\omega$.

A precise plasma measurement therefore requires calculating the antenna impedance $Z = R + 1/iC\omega$, from which one deduces the receiver gain

$$\Gamma^2 = \frac{V^2}{V_R^2} = \left(\frac{C + C_B}{C}\right)^2 + (RC_B\omega)^2 \tag{37}$$

The antenna impedance is given by [*Meyer-Vernet and Perche*, 1989]

$$Z = \frac{4i}{\pi^2\varepsilon_0\omega}\int_0^\infty dk\,\frac{F(kL)F_a(ka)}{\varepsilon_L} \tag{38}$$

where the function F is given in (4) or (5), and F_a takes into account the finite radius a of the antenna as

$$F_a(x) = J_0^2(x) \qquad \text{wires}$$

$$F_a(x) = \left[\frac{\sin x}{x}\right]^2 \qquad \text{spheres}$$

Indeed, although for $a/L_D \ll 1$, both the real part of Z and V^2 can be calculated by using the approximation $F_a(x) = 1$ as we did in the previous sections, this is not so for the imaginary part of Z since the capacitance depends on the field at distance a, so that one cannot use the limit $ka \to 0$ [*Meyer-Vernet and Perche*, 1989].

For sufficiently small values of a/L_D, Γ^2 exhibits a rather smooth variation, except if one has simultaneously $\omega \approx \omega_p$ and $L/L_D > 10$ [*Couturier et al.*, 1981]. In the latter case, the fine structure of the peak of the spectrum might be affected by the antenna impedance Z. Note, however, that one expects that Z should not depend very much on the high-energy electrons, except through their contribution to the low-order moments.

In particular, it is easy to transpose to the resistance R the analytical results obtained for V^2, by noting that R (from (38)) is calculated by replacing $B(k)$ in (1) by the quantity

$$\frac{k^2\,\mathrm{Im}\,\varepsilon_L}{4\pi m\omega\omega_p^2} = \frac{\pi f(\omega/k)}{2mk}$$

Consequently, for low frequencies the analytical values for R are trivially deduced by replacing the integral $\int_0^\infty dvvf(v)$ in (15), (16), and (18) by the quantity $f(0)/(4m)$.

For high frequencies, R is given by (19), where the integral over v is replaced by $f(\omega/k)/(4m)$. Using as in section 3.2 the approximations of F for large arguments (13) or (14) and making the change of variable $v = \omega/k$, we obtain instead of (21) and (22)

$$R \approx \frac{\omega_p^2}{2\varepsilon_0 L\omega^3} \qquad L/L_D \gg 1 \quad \text{(wires)} \tag{39}$$

$$R \approx \frac{2\pi\omega_p^2}{\varepsilon_0\omega^2}\int_0^\infty dvvf(v) \qquad L/L_D \gg 1 \quad \text{(spheres)} \tag{40}$$

An interesting point is that the high-frequency resistance of a long wire dipole antenna is independent of the distribution function: it only depends on the total electron density.

In the vicinity of the plasma frequency, R is given by (27) for long antennae, where $B(k_0)$ is to be replaced by $\pi f(\omega/k_0)/(2mk_0)$, and thus

$$R \approx \frac{2\omega_p F(k_0L)}{\pi\varepsilon_0\langle v^2\rangle k_0} \qquad L/L_D \gg 1 \tag{41}$$

We find therefore that in contrast to the noise spectrum, the resistance does not depend crucially on the high-energy electrons (except if they contribute significantly to the pressure), even near ω_p. This confirms the results previously obtained in the particular case of distributions made of several Maxwellians.

4. "KAPPA" DISTRIBUTION FUNCTION

4.1. *Choice of the Distribution Function*

We choose the following electron velocity distribution function:

$$f_\kappa(v) = \frac{A}{(1 + v^2/\kappa v_0^2)^{\kappa+1}} \tag{42}$$

Such f_κ functions will be named in this paper "kappa functions"; κ is a real number larger than or equal to 2, but in order to simplify future calculations we will only consider integer values of κ.

These functions were introduced to describe the departure of actual electron distributions from Maxwellians in the interplanetary medium and the Earth's magnetosphere [see *Olbert, 1968; Vasyliunas*, 1968; *Binsack*, 1966].

From the experimenter's point of view, these functions are very interesting, since although they have only two adjustable parameters, they are rather close to a Maxwellian at low velocities, while they join smoothly onto a power law spectrum at high energies. The fitting of energy spectra measured in the Earth's plasma sheet gave approximate values $\kappa \sim 2$–4 [*Vasyliunas*, 1968]. In the solar wind, values $\kappa \sim 4$–7 (J. D. Scudder, private communication, 1989) seem to describe rather well the core-halo parameterization used by *Feldman et al.* [1975].

From the theorist's point of view, the kappa functions have the interest of being analytically easily tractable. As is well known, they reduce to a Maxwellian distribution in the limit $\kappa \to \infty$.

A convenient indicator for deviations of a distribution function from a superposition of Maxwellians might be the differential temperature used by *Pilipp et al.* [1987],

$$T_{\text{diff}} = -\left(k_B\frac{d\ln f}{dE}\right)^{-1}$$

($E = mv^2/2$). For a Maxwellian at temperature T, $T_{\text{diff}} = T$. For a superposition of two Maxwellians ("cool" and "hot"), $T_{\text{diff}} = T_C$ at low energies but increases to T_H at larger energies and remains constant. On the other hand, for kappa distributions we find

$$T_{\text{diff}} = \frac{mv_0^2}{2k_B}\,\frac{\kappa + v^2/v_0^2}{\kappa + 1}$$

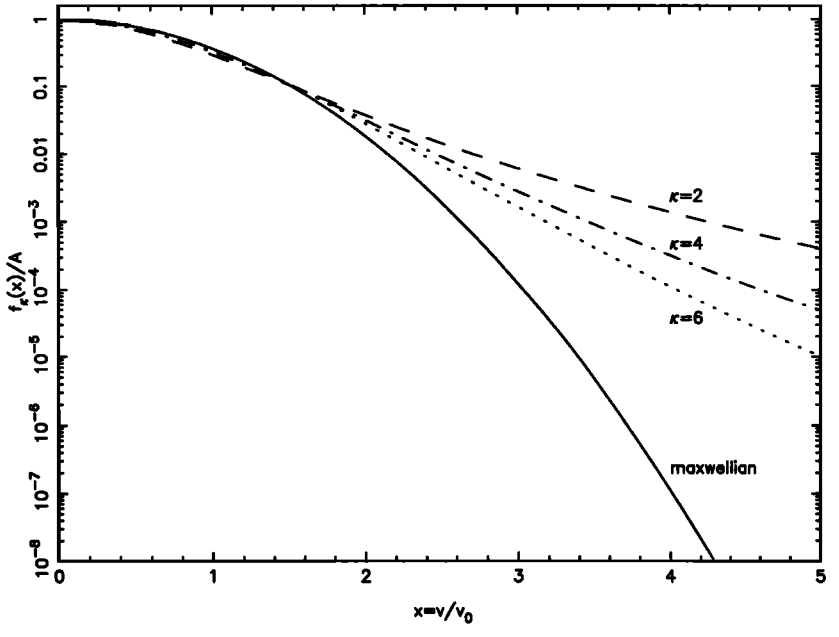

Fig. 1. Comparison between the "kappa" distribution functions corresponding to the values of κ used in this paper and their Maxwellian limit ($\kappa \to \infty$). Here the functions have been normalized so that $f(0) = 1$.

Thus T_{diff} is constant at low energies, as for a Maxwellian, but increases monotonically at larger energies. This behavior seems in qualitative agreement with the differential temperature calculated on the basis of isotropic distribution functions measured in the solar wind [see *Pilipp et al.*, 1987, Figure 5*c*].

Figure 1 shows a set of such functions compared to their Maxwellian limit.

Let us first calculate the moments of $f(v)$ defined in (7). We get

$$\langle v^n \rangle = 2\pi A (v_0 \kappa^{1/2})^{n+3} \Gamma\left(\frac{n+3}{2}\right) \Gamma\left(\kappa - \frac{n+1}{2}\right) \cdot [\Gamma(\kappa+1)]^{-1} \quad (43)$$

where $\Gamma(x)$ denotes the gamma function. Since the distribution function is normalized as $\langle v^0 \rangle = 1$, we find quite immediately the value of A:

$$A = \frac{\Gamma(\kappa+1)}{(\pi\kappa)^{3/2} v_0^3 \Gamma(\kappa - 1/2)}$$

We can also calculate the equivalent temperature $T = m\langle v^2 \rangle / 3k_B$; using (43) and properties of the gamma function, we obtain

$$T = \frac{m v_0^2}{k_B} \frac{\kappa}{2\kappa - 3} \quad (44)$$

As said above, we only consider integer values of κ. In this case, A becomes

$$A = \frac{2^{\kappa-1} \kappa!}{\pi^2 v_0^3 \kappa^{3/2} (2\kappa - 3)!!} \quad (45)$$

where

$$\kappa! = 1 \times 2 \times 3 \times \cdots \times (\kappa - 1) \times \kappa$$

$$(2\kappa - 3)!! = 1 \times 3 \times 5 \times \cdots \times (2\kappa - 5) \times (2\kappa - 3)$$

4.2. *Longitudinal Dielectric Permittivity*

The longitudinal dielectric permittivity is given by (3). Replacing $f(v)$ by the kappa function, we obtain

$$\varepsilon_L = 1 + \frac{2\pi\omega_p^2}{k} A \cdot \int_{-\infty}^{+\infty} dv_\parallel \frac{v_\parallel}{(kv_\parallel - \omega - io)(1 + v_\parallel^2/\kappa v_0^2)^{\kappa+1}}$$

Setting $x = v_\parallel / \kappa^{1/2} v_0$ and $z = \omega / \kappa^{1/2} k v_0$, we get

$$\varepsilon_L = 1 + \frac{2\pi\omega_p^2}{k^2} (I_1 + z I_2) \quad (46)$$

with

$$I_1 = A v_0 \kappa^{1/2} \int_{-\infty}^{+\infty} \frac{dx}{(x^2+1)^{\kappa+1}} \quad (47)$$

$$I_2 = A v_0 \kappa^{1/2} \int_{-\infty}^{+\infty} \frac{dx}{(x - z - io)(x^2+1)^{\kappa+1}} \quad (48)$$

The calculation of I_1 is straightforward and gives

$$I_1 = \frac{1}{\pi v_0^2} \frac{\kappa - 1/2}{\kappa} \quad (49)$$

Calculating I_2 is equivalent to integrating the function

$$\frac{1}{(x-z)(x^2+1)^{\kappa+1}} \tag{50}$$

on the real axis avoiding the real pole $x = z$ by passing below it. To achieve the calculation of I_2, the integration path is closed with a large semicircle in the half complex plane Im $x < 0$. The contribution of the integration on this large semicircle is zero because

$$\left|\frac{x}{(x-z)(x^2+1)^{\kappa+1}}\right| \to 0 \qquad |x| \to \infty$$

The only pole included inside the integration path is $-i$. So

$$I_2 = A v_0 \kappa^{1/2} (-2i\pi) R$$

where R is the residue of the function (50) for the pole $-i$. We have

$$R = \frac{1}{\kappa!}\frac{d^\kappa}{dx^\kappa}\left(\frac{1}{(x-z)(x-i)^{\kappa+1}}\right) \qquad x = -i$$

Using Leibnitz's formula, we write

$$\frac{d^\kappa}{dx^\kappa}\left(\frac{1}{(x-z)(x-i)^{\kappa+1}}\right) = \sum_{p=0}^{\kappa} C_\kappa^p \frac{d^p}{dx^p}\left(\frac{1}{(x-i)^{\kappa+1}}\right)\frac{d^{\kappa-p}}{dx^{\kappa-p}}\left(\frac{1}{x-z}\right)$$

with

$$C_\kappa^p = \frac{\kappa!}{p!(\kappa-p)!}$$

$$\frac{d^n}{dx^n}\left(\frac{1}{x-z}\right) = (-1)^n \frac{n!}{(x-z)^{n+1}}$$

$$\frac{d^n}{dx^n}\left(\frac{1}{(x-i)^{\kappa+1}}\right) = (-1)^n \frac{(\kappa+n)!}{\kappa!}\frac{1}{(x-i)^{\kappa+1+n}}$$

and we obtain eventually

$$R = \frac{(-1)^\kappa}{\kappa!}\sum_{p=0}^{\kappa}\frac{(\kappa+p)!}{p!}\frac{1}{(2i)^{\kappa+1+p}(z+i)^{\kappa+1-p}}$$

We can now deduce the final expression of ε_L:

$$\varepsilon_L = 1 + \frac{z^2}{r^2}\left(2\kappa - 1 + \frac{(-2)^{\kappa+1}}{(2\kappa-3)!!}iz \cdot \sum_{p=0}^{\kappa}\frac{(\kappa+p)!}{p!}\frac{1}{(2i)^{\kappa+1+p}(z+i)^{\kappa+1-p}}\right) \tag{51}$$

where $r = \omega/\omega_p = f/f_p$.

The dielectric function has the low-frequency limit

$$\varepsilon_L \to 1 + \frac{z^2}{r^2}(2\kappa-1) = 1 + \left(\frac{\omega_p}{k v_0}\right)^2 \frac{2\kappa-1}{\kappa} \qquad \omega \to 0$$

Comparing this with the corresponding limit for a Maxwellian distribution, namely

$$\varepsilon_L \to 1 + \frac{1}{k^2 L_D^2}$$

which means that the low-frequency electric perturbations are exponentially shielded over a distance L_D, we define the Debye length in this plasma as

$$L_D = \frac{v_0}{\omega_p}\left(\frac{\kappa}{2\kappa-1}\right)^{1/2} \tag{52}$$

Note that by replacing v_0 by its expression (44) as a function of the equivalent temperature T, we obtain

$$L_D = \frac{1}{\omega_p}\left(\frac{k_B T}{m}\frac{2\kappa-3}{2\kappa-1}\right)^{1/2} \tag{53}$$

so that the Debye length depends not only on ω_p and T but also on κ. Of course, for $\kappa \to \infty$, we recover the usual Maxwellian result $L_{D_{maxw}}$.

4.3. *Calculation of the Electrostatic Noise*

The fluctuations of the electrostatic field are given in (1). The dielectric function ε_L has just been calculated and is given by (51). $F(kL)$ depends on the geometry of the antenna: depending on whether the antenna is a wire dipole or a dipole made of two spheres, expression (4) or (5) has to be used. Let us now calculate $B(k)$.

Inserting (42) into (2), we get

$$B(k) = \frac{2\pi A}{k}\int_{\omega/k}^{+\infty} dv \frac{v}{(1 + v^2/\kappa v_0^2)^{\kappa+1}}$$

which gives, after we set $x = v^2/\kappa v_0^2$ and $z = \omega/\kappa^{1/2} k v_0$,

$$B(k) = \frac{2\pi A}{k}\frac{\kappa v_0^2}{2}\int_{z^2}^{+\infty}\frac{dx}{(1+x)^{\kappa+1}}$$

This is trivially integrated as

$$B(k) = \frac{\pi A v_0^2}{k}\frac{1}{(1+z^2)^\kappa} \tag{54}$$

Substituting this expression of $B(k)$ into (1) and setting $z = \omega/\kappa^{1/2} k v_0$, $r = \omega/\omega_p$, and $u = L/L_D$ with L_D given by (52), we obtain

$$V^2 = \frac{2^{\kappa+3}}{\pi^2 \varepsilon_0}\frac{\kappa!}{(2\kappa-3)!!\kappa^{1/2}}\frac{m v_0}{r^2}\int_0^{+\infty} dz\, zF\left(\frac{ru}{z(2\kappa-1)^{1/2}}\right) \cdot [(1+z^2)^\kappa |\varepsilon_L|^2]^{-1} \tag{55}$$

Introducing the equivalent temperature given by (44), we find the expression of the normalized fluctuations

$$\frac{V^2}{T^{1/2}} = \frac{2^{\kappa+3}}{\pi^2\varepsilon_0}(k_B m)^{1/2}\frac{(\kappa-1)!(2\kappa-3)^{1/2}}{(2\kappa-3)!!}\frac{1}{r^2} \cdot \int_0^{+\infty} dz\, zF\left(\frac{ru}{z(2\kappa-1)^{1/2}}\right)[(1+z^2)^\kappa|\varepsilon_L|^2]^{-1} \tag{56}$$

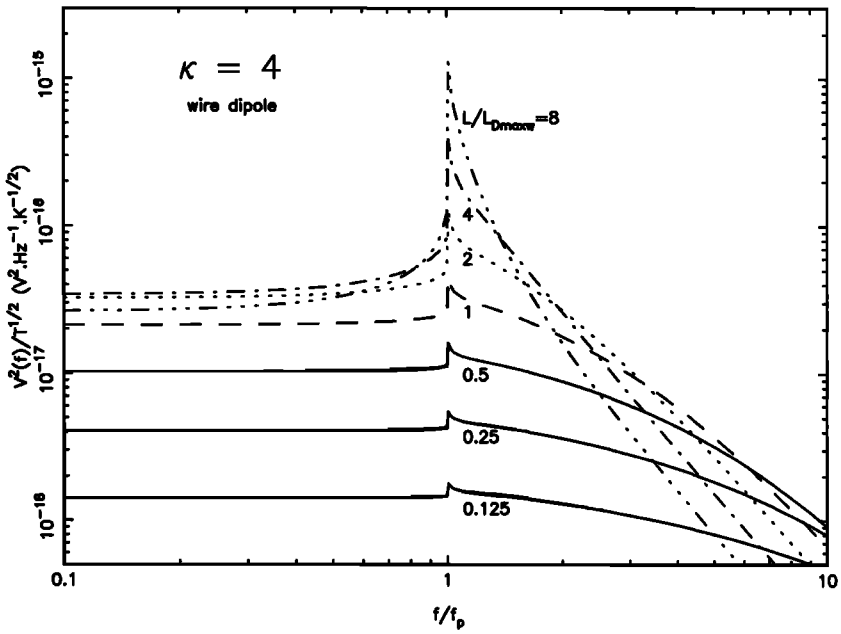

Fig. 2. Noise power spectrum in V^2 Hz^{-1} normalized to $T(K)^{1/2}$ calculated with a "kappa" electron distribution ($\kappa = 4$) and a wire dipole antenna for different values of the normalized antenna length $L/L_{D_{maxw}}$.

keeping in mind that ε_L is given in (51).

As the analytic calculation of $V^2T^{-1/2}$ cannot be done in general, the integration must be numerically computed. This is easier than for a Maxwellian distribution since the dielectric permittivity ε_L does not involve any special function.

The comparison between the spectra corresponding to kappa distribution functions and those corresponding to other distributions must be done for the same values of the equivalent temperature. Yet L_D depends not only on the temperature but also on κ (see equation (53)). That is why spectra shown in the figures have been drawn not for different values of $u = L/L_D$ but for different values of $u = L/L_{D_{maxw}}$ where $L_{D_{maxw}}$ (defined in (11)) is the value of L_D for a Maxwellian distribution with the same equivalent temperature so that it now depends only on T (and ω_p and L) but no longer on κ. Using (11) and the equivalent temperature given by (44), we have

$$L_{D_{maxw}} = \frac{v_0}{\omega_p}\left(\frac{\kappa}{2\kappa - 3}\right)^{1/2}$$

so that the only thing you have to do is to replace $F[ru/z(2\kappa - 1)^{1/2}]$ by $F[ru/z(2\kappa - 3)^{1/2}]$ in the expression of $V^2/T^{1/2}$ to achieve the calculation as a function of the parameter $u = L/L_{D_{maxw}}$.

5. Results and Discussion

In order to study how the shape of the distribution function determines the quasi-thermal noise spectrum, we will first compare spectra calculated with different values of κ and then compare them with Maxwellian, "flat-top," or bi-Maxwellian distributions. Of course, we consider plasmas having the same density and equivalent temperature, so that the curves are drawn using the parameter $L/L_{D_{maxw}}$. In calculating these curves we have excluded the spectral region where $1 < \omega/\omega_p < 1.01$, because it presents some numerical difficulties and, in any case, the usual noise receivers have a bandwidth of the order of 1% or more. The limitation due to relativistic velocities discussed in section 3.3 is then irrelevant if the equivalent plasma temperature is smaller than about 4×10^7 K (because X_m is then smaller than 1%). Note that from equation (36) the mean of the spectrum over the frequency range $\omega/\omega_p = 1$ and $\omega/\omega_p = 1.01$ is about 2 times the value for $\omega/\omega_p = 1.01$.

Figures 2 and 3 show a set of normalized spectra calculated with a kappa distribution $\kappa = 4$ for different values of the parameter $L/L_{D_{maxw}}$ and a wire dipole and a double-sphere antenna, respectively. This illustrates the generic behavior of quasi-thermal noise spectra: a plateau below f_p, a cutoff at f_p with a peak which is sharper for long antennae, and a high-frequency spectrum proportional to f^{-3} or f^{-2} for wire or sphere long dipole antennae, respectively; on the other hand, the spectrum is nearly flat for short antennae. As shown in section 3.3, the peak is sharp and occurs at f_p, which is a generic property of distributions having a power law tail.

Figure 4 shows the effect of changing the parameter κ. Here we have compared $\kappa = 2$, 4, and 6, for a short wire dipole antenna ($L/L_{D_{maxw}} = 0.5$) and a long one ($L/L_{D_{maxw}} = 8$). Other cases are given by *Chateau* [1991]. The low-frequency level depends on the low-order moments of the distribution (and more strongly for longer antennae), but these moments do not depend very much on κ for $\kappa \gg 1$: note for instance that for $\kappa = 2$, $L_D = L_{D_{maxw}}/3^{1/2}$, while for $\kappa \geq 4$, L_D differs from $L_{D_{maxw}}$ by less than 15%. This is why the curves $\kappa = 4$ and 6 are near each other but rather different from $\kappa = 2$.

On the other hand, for long antennae the differences near f_p stem from the high-energy tail, which varies as $1/v^{2\kappa+2}$; the peaks for the different values of κ behave as in (36). Note also that if there are more high-energy electrons, the spectrum just below f_p is higher, so that the cutoff is rounded off; this is clearly seen for the curve $\kappa = 2$. We also verify that

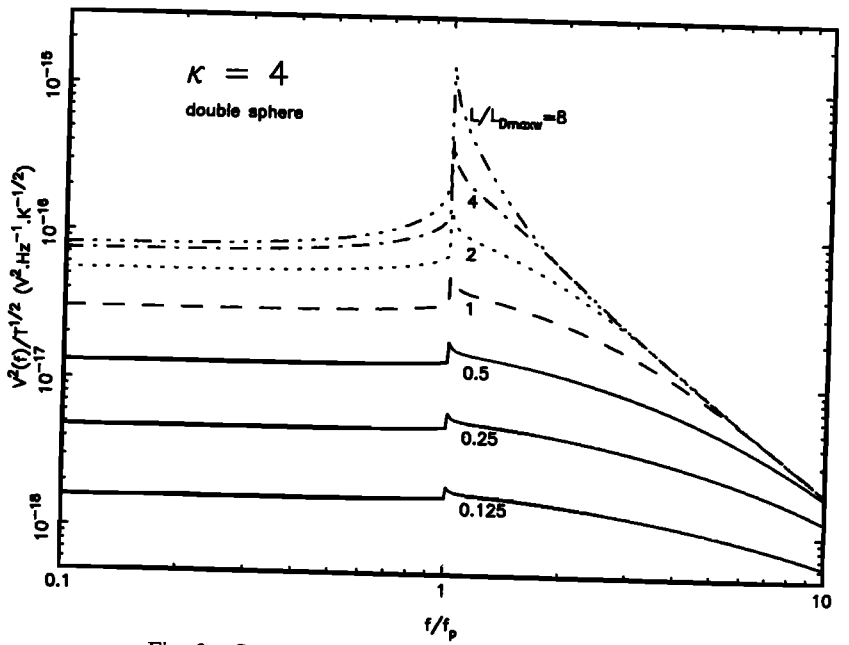

Fig. 3. Same as Figure 2 for a double-sphere antenna.

for a long wire dipole antenna the high-frequency level depends not on κ, but only on n and T.

In Figure 5, we compare three cases: a kappa distribution ($\kappa = 3$), a Maxwellian, and a "flat top," for a short wire dipole antenna ($L/L_{D_{maxw}} = 0.5$) and a long one ($L/L_{D_{maxw}} = 8$). The flat-top distribution $f(v) \propto 1/1 + (v/v_0)^8$ was studied by *Chateau and Meyer-Vernet* [1989]; it has a flat top at low energies and a power law tail $\propto v^{-8}$. It is thus interesting to compare the results with a $\kappa = 3$ distribution whose high-energy tail has the same form. We note the following points, illustrating the generic properties. First, we see again that the high-frequency levels for a long dipole antenna are identical, since they depend only on n and T.

Second, the peaks are identical for the kappa and the flat top, as expected from (36) since their high-energy tails have the same power law variation. Note, however, an interesting point; though both tails vary as v^{-8}, they are not equal: for $v/\langle v^2 \rangle^{1/2} \gg 1$, $f(v)$ is a factor $8/(2 + 2^{1/2})^{1/2}$ larger for $\kappa = 3$ than for the flat top, yet the peaks are identical. This is because the noise peak has the form $V_0^2 \propto B(k_0)/f(\omega/k_0)$ (see (27)), so that only the shape of the tail (for velocities $v > v_\omega$) matters, not its amplitude. Note also that as shown in section 3.3, the Maxwellian distribution produces a very different peak: it is much broader and occurs significantly above f_p.

Third, the low-frequency levels are slightly different, due to the difference in the low-energy electrons. A final point is

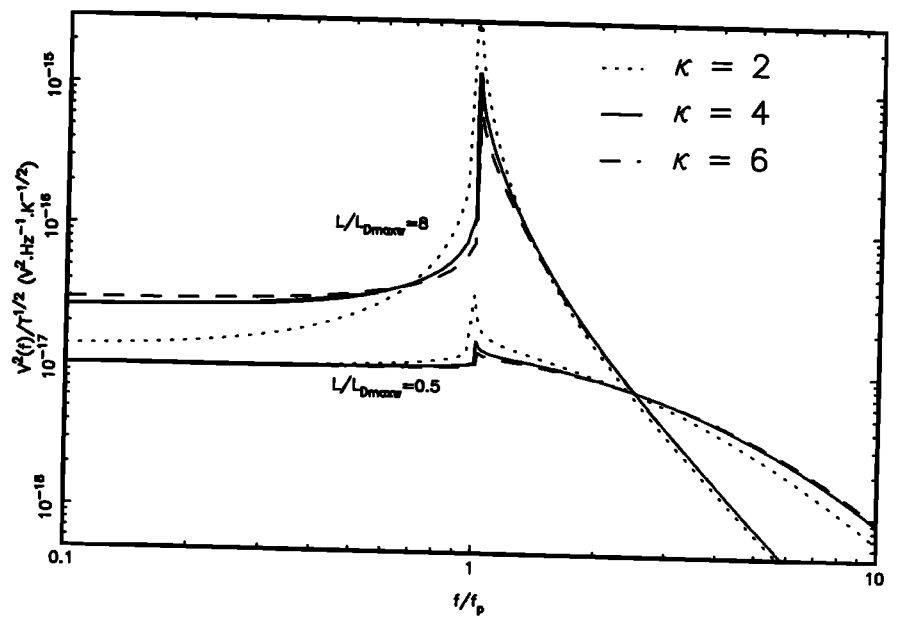

Fig. 4. Noise power spectrum in V^2 Hz^{-1} normalized to $T(K)^{1/2}$, calculated with "kappa" electron distributions $\kappa = 2$, 4, and 6, with two different values of the normalized length $L/L_{D_{maxw}}$ of a wire dipole antenna.

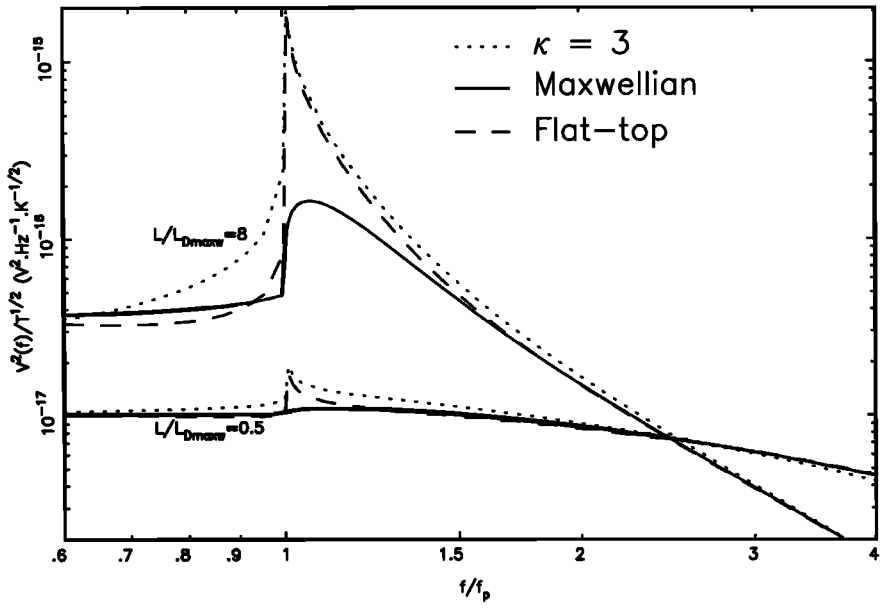

Fig. 5. Comparison between the spectra (normalized to $T^{1/2}$) calculated with a "kappa" distribution $\kappa = 3$, a Maxwellian, and a "flat top," for two different values of the normalized length $L/L_{D_{maxw}}$ of a wire dipole antenna.

worth noting: although the function $\kappa = 3$ and the flat top produce the same f_p peaks, the former gives a much larger noise level just below f_p. This is because this level, in contrast to the peak, depends on the quantity of electrons in the high-energy tail (not only on the shape of the tail), and the function $\kappa = 3$ has a much larger proportion of high-energy electrons than the flat top. On the other hand, we see that the Maxwellian, which has practically no high-energy ($v \gg \langle v^2 \rangle^{1/2}$) electrons, yields a spectrum with a very sharp cutoff.

High-energy electrons are often described by adding to a (cold) Maxwellian distribution a second (hot) Maxwellian; this kind of modeling has been used to compute quasi-thermal noise spectra [see *Couturier et al.*, 1981]. In Figure 6 we have compared a spectrum calculated with a sum of Maxwellians ($n_H/n_C = 0.01$, $T_H/T_C = 10$), with our results for a kappa ($\kappa = 4$) and a flat top distribution for a long wire dipole antenna of length $L/L_{D_{maxw}} = 8$; these parameters are rather typical in the solar wind. In order to illustrate a case with more high-energy electrons, Figure 7 compares a bi-Maxwellian having $n_H/n_C = 0.01$, $T_H/T_C = 100$, with our results for $\kappa = 2$.

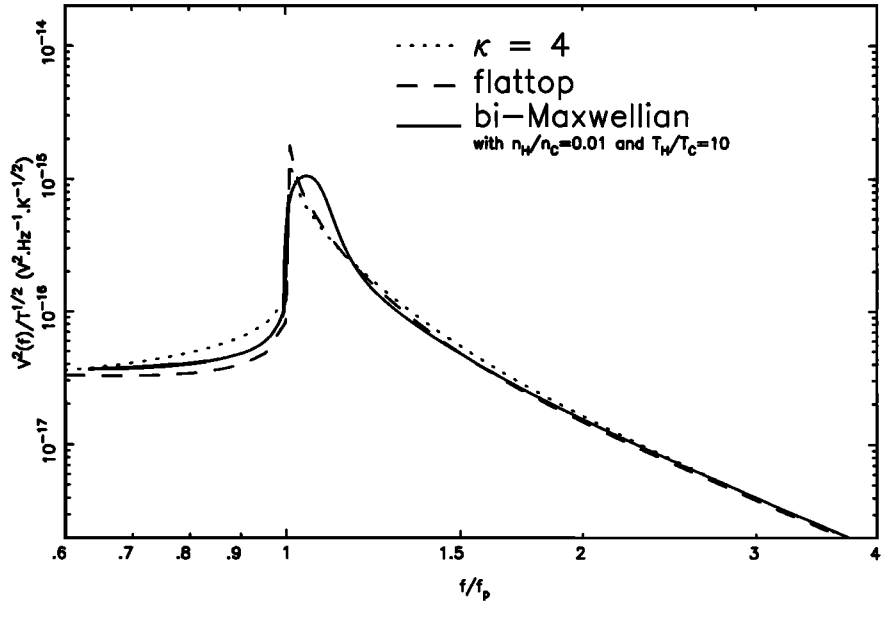

Fig. 6. Comparison of the spectra obtained with a "kappa" distribution $\kappa = 4$, a distribution made of a cold and a hot Maxwellian with $n_H/n_C = 0.01$ and $T_H/T_C = 10$, and a "flat top," for a wire dipole antenna of length $L/L_{D_{maxw}} = 8$.

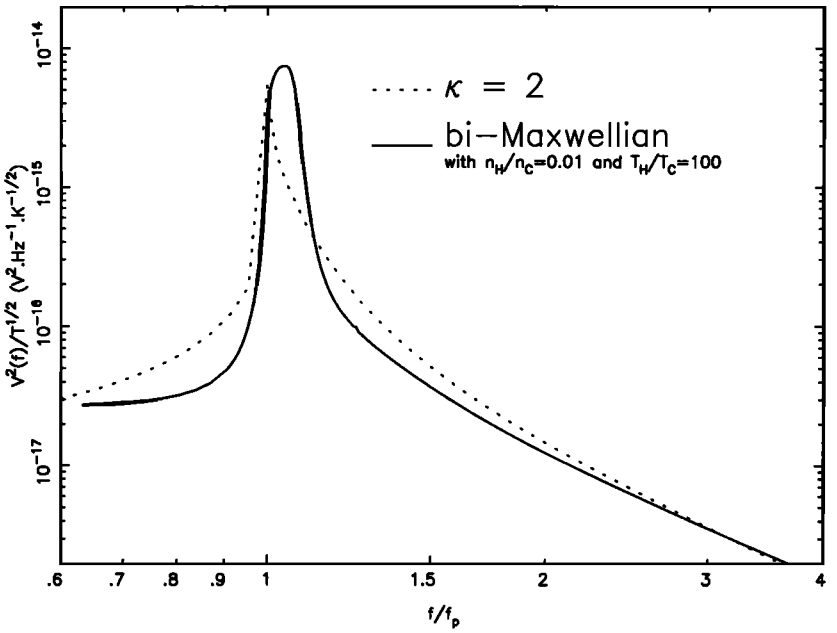

Fig. 7. Comparison of the spectra calculated with a "kappa" distribution $\kappa = 2$, and with a bi-Maxwellian having $n_H/n_C = 0.01$ and $T_H/T_C = 100$, for a wire dipole antenna of length $L/L_{D_{maxw}} = 8$.

Two important points are worth noting. First, the bi-Maxwellian noise spectra have a peak which is above f_p and less sharp than that obtained with the other functions: as already discussed, this is a generic feature of Maxwellian tails, as compared to power law ones. Second, the kappa functions produce higher levels just below f_p than the other distributions, which reflects the fact that they have more high-energy electrons; this smooths the cutoff. On the other hand, the flat top, which has few high-energy electrons (even though the tail varies as v^{-8}) has a low level of noise just below f_p and thus a sharp cutoff. It is important to note, however, that, as discussed by *Chateau and Meyer-Vernet* [1989], these differences are not very important, so that a rather sensitive experiment is necessary to detect them.

6. Conclusions

We have derived the following generic properties of the electrostatic noise in a stable isotropic plasma of density n and equivalent electron temperature T (proportional to the mean square velocity, as defined in (8)).

1. The high-frequency ($f \gg f_p$) noise level on an antenna of length $L \gg L_D$ varies as

$$V^2(\mathrm{V^2\ Hz^{-1}}) \approx 4 \times 10^{-11} T(\mathrm{K}) n(\mathrm{m^{-3}})/f^3(\mathrm{Hz}) L(\mathrm{m})$$

for a wire dipole and as $V^2 \propto n\langle v\rangle/\omega^2$ for a double sphere (see (23) and (24)). Therefore the measurement of this level gives a direct determination of either the pressure or the flux, for any stable distribution function. This result might provide a practical method for measuring one of these quantities at a high rate in space, without having to measure a complete frequency spectrum.

2. The low-frequency level ($f \ll f_p$) has a plateau which depends on the low-order moments of the velocity distribution function, e.g., equations (15), (16), and (18). In practice, with either kappa distributions having $\kappa \geq 4$ or flat-top distributions (for which the hot electrons do not contribute too much to the equivalent temperature T), this plateau differs from the Maxwellian result by less than about 20%, for practical antenna lengths. In particular, the usual analytic expression V^2 ($\mathrm{V^2\ Hz^{-1}}$) $\approx 3.5 \times 10^{-14}$ $T(\mathrm{K})/L(\mathrm{m}) n^{1/2}$ ($\mathrm{m^{-3}}$) [*Meyer-Vernet and Perche*, 1989] may still be used to obtain an order of magnitude of the equivalent temperature with long wire dipole antennae. If, however, one has a long wire dipole antenna with a sensitive and well-calibrated receiver measuring the whole spectrum, one can first determine n and T precisely from the cutoff and the high-frequency level; then the spectrum below f_p can be used to determine the distribution function at low energies. This might have important applications since the usual electron analyzers have much difficulty in determining low-energy electron parameters.

3. For most practical distributions the peak of the spectrum has a cutoff which determines the plasma frequency, and thus the total electron density. The peak shape strongly depends on the distribution of the high-energy electrons. For a power law tail the peak is nearly exactly at the plasma frequency (in contrast to what happens with a Maxwellian tail). However, the measurement of the high-energy electrons is generally limited by the finite frequency resolution $\Delta\omega/\omega$ of the noise receiver, since the peak cannot give any information on the electrons of velocity $v \geq [\langle v^2\rangle/(2\Delta\omega/\omega)]^{1/2}$, except if these electrons contribute to the pressure in an important way.

One might think naively that the fine structure of the peak could be resolved by using a receiver with a sufficient frequency resolution. This is not necessarily true, however, since in practice the spectrum is acquired over a finite time, during which the plasma density fluctuates. When these density fluctuations occur at frequencies much smaller than

the plasma frequency, the noise peak fluctuates accordingly. Since $f_p \propto n^{1/2}$, the observed peak should be broadened by one-half the amplitude of the density fluctuations $\Delta n/n$.

For instance, it is well known that in the free solar wind the electron density fluctuations are usually of the order of a few percent, on time scales larger than a few seconds. Consequently, over such time scales the peak cannot be determined with a resolution better than 1%; this precludes any fine measurement of electrons of velocity larger than about 7 times the mean square velocity, by thermal noise spectroscopy, at such time scales in the solar wind (except if these electrons contribute significantly to the pressure).

This is not, however, the whole story, because the above quoted value does not take into account the fluctuations over shorter time scales, for which the measurements are much more difficult. *Celnikier et al.* [1987] have found that the power spectrum of the electron density fluctuations in the solar wind near 1 AU decreases with a power law index generally smaller than 1 for time scales between about 0.06 s and 15 s. A similar flattening with respect to a Kolmogorov spectrum has been found nearer the Sun [*Coles and Harmon*, 1989]. This means that short time scales play a dominant role in the calculation of $\Delta n/n$, so that the value of a few percent quoted above is clearly an underestimate: for instance, the fluctuation spectrum obtained by *Celnikier et al.* [1987] gives $\Delta n/n \approx 5\%$ when it is integrated between 0.06 s and 6 s. Consequently, a noise peak acquired in about 6 s should be broadened by about 3%, or perhaps more since the contribution of time scales shorter than 0.06 s is presently unknown.

Can we deduce practical consequences for interpreting noise spectra measured with past or present experiments in space? They generally have either a low-frequency resolution or a large integration time or both. For instance, the radio experiment aboard ISEE 3 has a frequency resolution barely better than 10% near the plasma frequency in the solar wind [*Knoll et al.*, 1978]. Aboard ISEE 1 and 2 the noise receiver, which has a better frequency resolution, acquires a noise spectrum in 4 s at its highest rate [*Harvey et al.*, 1978]. Either of these effects should round off the peak and, owing to its dissymmetry, should shift it above the plasma frequency. This would make the peaks of the curves shown in Figure 6 nearly indistinguishable in practice. As a consequence, an attempt to deduce high-energy tails by thermal noise spectroscopy with such experiments might give meaningless results in some cases; for example, in the case of a receiver having poor frequency or time resolution and a plasma with a power law tail, one could obtain a quite irrelevant hot electron temperature by fitting to the measured spectrum one constructed from a sum of Maxwellians. However, such an experiment can nevertheless give reliable results for the bulk of the distribution (i.e., $v \gg \langle v^2 \rangle^{1/2}$) if it uses a long wire dipole antenna.

On the other hand, the future experiments planned aboard Wind or CRAF might allow one to distinguish between kappa distributions and distributions made of two Maxwellians in the solar wind if they have a frequency resolution of the order of 1% and a time resolution better than a fraction of a second.

Finally, it is important to note that the results obtained in this paper rest on two important assumptions: the isotropy of the electron distribution and the absence of ambient static magnetic field. Although reliable results have been obtained with these assumptions in both the solar wind and a cometary environment, and some hints have been given about the effects of relaxing these assumptions (see, for instance, references given by *Meyer-Vernet and Perche* [1989]), more studies of the effect of the magnetic field might be needed for fully interpreting noise spectra that will be measured aboard the space probe Ulysses [*Stone et al.*, 1983], which (hopefully) will pass through the Io torus near Jupiter before exploring the Sun's polar regions, or aboard the projected Cassini spacecraft near the planet Saturn.

Acknowledgments. The Editor thanks two referees for their assistance in evaluating this paper.

REFERENCES

Binsack, J. H., Plasma studies with the IMP-2 satellite, Ph.D. thesis, Mass. Inst. of Technol., Cambridge, 1966.

Celnikier, L. M., L. Muschietti, and M. V. Goldman, Aspects of interplanetary plasma turbulence, *Astron. Astrophys.*, *181*, 138, 1987.

Chateau, Y. F., Theoretical study of the electrostatic field fluctuation spectrum in non-Maxwellian plasmas, doctoral thesis, Univ. Paris 6, 1991.

Chateau, Y. F., and N. Meyer-Vernet, Electrostatic noise in non-Maxwellian plasmas: "Flat-top" distribution function, *J. Geophys. Res.*, *94*, 15,407, 1989.

Coles, W. A., and J. K. Harmon, Propagation observations of the solar wind near the Sun, *Astrophys. J.*, *337*, 1023, 1989.

Couturier, P., S. Hoang, N. Meyer-Vernet, and J. L. Steinberg, Quasi-thermal noise in a stable plasma at rest, *J. Geophys. Res.*, *86*, 11,127, 1981.

Feldman, W. C., J. R. Asbridge, S. J. Bame, M. D. Montgomery, and S. P. Gary, Solar wind electrons, *J. Geophys. Res.*, *80*, 4181, 1975.

Harvey, C. C., J. Etcheto, Y. de Javel, R. Manning, and M. Petit, The ISEE electron density experiment, *IEEE Trans. Geosci. Electron.*, *GE-16*, 231, 1978.

Knoll, R., G. Epstein, S. Hoang, G. Huntzinger, J. L. Steinberg, J. Fainberg, F. Grena, S. R. Mosier, and R. G. Stone, The 3-dimensional radio mapping experiment (SBH) on ISEE-C, *ISEE Trans. Geosci. Electron.*, *GE-16*, *199*, 1978.

Meyer-Vernet, N., and C. Perche, Tool kit for antennae and thermal noise near the plasma frequency, *J. Geophys. Res.*, *94*, 2405, 1989.

Olbert, S., Summary of experimental results from M.I.T. detector on IMP-1, in *Physics of the Magnetosphere*, edited by R. L. Carovillano et al., p. 641, D. Reidel, Norwell, Mass., 1968.

Pilipp, W. G., H. Miggenrieder, M. D. Montgomery, K. H. Mühlhäuser, H. Rosenbauer, and R. Schwenn, Characteristics of electron velocity distribution functions in the solar wind derived from the Helios plasma experiment, *J. Geophys. Res.*, *92*, 1075, 1987.

Sitenko, A. G., *Electromagnetic Fluctuations in Plasma*, Academic, San Diego, Calif., 1967.

Stone, R. G., et al., The ISPM Unified Radio and Plasma Wave Experiment, *Eur. Space Agency Spec. Publ.*, *ESA SP-1050*, 187, 1983.

Vasyliunas, V. M., A survey of low-energy electrons in the evening sector of the magnetosphere with OGO 1 and OGO 3, *J. Geophys. Res.*, *73*, 2839, 1968.

Y. F. Chateau and N. Meyer-Vernet, Recherche Spatiale, Observatoire de Paris, 92195 Meudon Cedex, France.

(Received April 30, 1990;
revised October 23, 1990;
accepted November 20, 1990.)